Nature Environment and Pollution Technology
An International Quarterly Scientific Journal

p-ISSN: 0972-6268
(Print copies up to 2016)
e-ISSN: 2395-3454

Vol. 22 | No. 4 | pp. 1891-1910 | 2023

Original Research Paper

https://doi.org/10.46488/NEPT.2023.v22i04.016

Open Access Journal

Heavy Metal Contamination Assessment in Sediments, Soils and Surface Waters in Agriculture-Based Rural Chhattisgarh, India, and Evaluation of Irrigation Water Quality

Manash Protim Baruah†*, Subhajit Das*, Monjil Rajkonwar and Mahesh Thirumala***
*Geological Survey of India, State Unit-Chhattisgarh, Raipur, India
**Department of Applied Geology, Dibrugarh University, Assam, India
†Corresponding author: Manash Protim Baruah; manashprotim.baruah@gsi.gov.in

Nat. Env. & Poll. Tech.
Website: www.neptjournal.com

Received: 10-04-2023
Revised: 14-06-2023
Accepted: 20-06-2023

Key Words:
Geochemical mapping
Stream sediments
Heavy metals
Contamination
Irrigation water

ABSTRACT

Regional geochemical mapping was carried out in Bilaspur and Korba Districts of Chhattisgarh, and stream sediments/slope wash, soil, and water samples were analyzed for concentration of heavy metals. The study contributes to understanding heavy metals contamination of sediments, soils, and water due to anthropogenic activity, mainly in agriculture-based rural areas. The study reveals that high geochemical anomalies observed for heavy metals like Ni, Cr, As, and Zn in sediments and soil samples are due to the extensive uses of phosphatic fertilizer and soil amendments in the form of poultry and swine manure. Water quality assessment of major streams in the study areas shows that the water is suitable for domestic and agricultural uses. Correlation analysis reveals that the chemical weathering of rock-forming minerals doesn't control the surface water chemistry of the study area and is also an anthropogenic source of sodium in water. This study also shows the importance of the country's geochemical mapping database, which will have much broader applications than conventional mineral exploration and geological mapping.

INTRODUCTION

Rapid urbanization, industrialization, and intensified agriculture in the recent past have increased undesirable environmental pollutants, including heavy metals. Increased concentrations of heavy metals, including Cr, Cu, Co, Cd, and Pb, in soils brought on by the use of agrochemicals and polluted irrigation water resulted in a decline in the health of the soil (Rayment et al. 2002, Kaur et al. 2014). Heavy metals are elements with metallic properties, a density of >5 g $cm^{-3,}$ and an atomic mass of >20 (Bakshi et al. 2018). According to He et al. (2015), the most prevalent heavy metals in the environment include arsenic (As), cadmium (Cd), chromium (Cr), copper (Cu), mercury (Hg), lead (Pb), and zinc (Zn), among others. Heavy metal contamination of agricultural soils and crops is a concern because it could impact human health and the viability of food production systems in contaminated areas.

These metals persist in the environment for a very long time. Half-lives for Cu are 310-1500 years, for Zn are 70-510 years, for Cd are 13-1100 years, and for Pb are 740-5900 years (Iimura et al. 1977), whereas the estimated residence times (in years) of 75-380 for Cd, 500-1000 for Hg and 1000-3000 for Cu, Ni, Pb and Zn under temperate climatic conditions (Kabata-Pendias 2011). Owing to their high residence periods, heavy metals tend to accumulate in soil and sediments and thus increase the toxic level of the biosphere (Chopra 2009). Heavy metals can be added to the environment through a variety of sources, which includes air that contains mining, smelting, and refining of fossil fuels; water having domestic sewage and industrial effluents; and soil like agricultural and animal wastes, municipal and industrial sewage, coal ashes, fertilizers, and pesticides. Heavy metal pollution often results in the degradation of soil health (Kools et al. 2005, Abdu et al. 2017), the contamination of surface and groundwater (Hashim et al. 2011, Mohankumar et al. 2016) and food chain pollution (Hapke 1996, Notten et al. 2005, Tchounwou et al. 2012), and consequently is a threat to human health (Pepper 2013, Jovanović et al. 2015, Oliver & Gregory 2015, Sarwar et al. 2017, Yang et al. 2017). Contrary to the pollution brought on by excessive levels of heavy metals in the soil, it has been documented in numerous regions of the world that agricultural lands are deficient in one or more micronutrients, including heavy metals/metalloids. This includes Cu, Mn, and Zn, which are essential for plants

and animals, and Co, Cr, and Se, which are necessary for animals.

Extensive studies of soil, stream sediment, and vegetation samples are done for mineral exploration due to the rising demand for metals and the need to find reserves for new ore minerals. Although originally developed for mineral exploration, stream sediment reconnaissance studies are particularly important for highlighting geochemical anomalies of importance to agriculture and showing regional soil pollution patterns. One such ambitious program launched by the Geological Survey of India, Ministry of Mines is the National Geochemical Mapping Program (NGCM) in 2001-2002. National Geochemical Mapping aims at mapping the country geochemically by sampling and analyses of stream sediment, soil, water, etc., intending to generate geochemical baseline data for multi-purpose uses like managing and developing natural resources, environmental management, agriculture, forestry, land use, and many aspects of human and animal health. As a part of this program, geochemical mapping was carried out for an area of 728 sq km in and around Kudri-Pasan in Bilaspur and Korba Districts of Chhattisgarh, India.

The study area falls in toposheet no.64J/01 and is bounded by latitudes 22°45' N to 23°00' N and longitudes 82°00' E to 82°15' E and forms parts of Bilaspur and Korba Districts of Chhattisgarh state (Fig. 1). Physiographically, the study area can be divided into three parts, viz. hilly terrain/dense forest, plantation/cultivated land and rivers/water bodies. The eastern part of the area has a rugged topography occupied by the sedimentary sequence of Lower Gondwana Formations. In contrast, the southwestern part is more or less a flat terrain with soil cover. The Sukhad and the Bamni nadi, along with

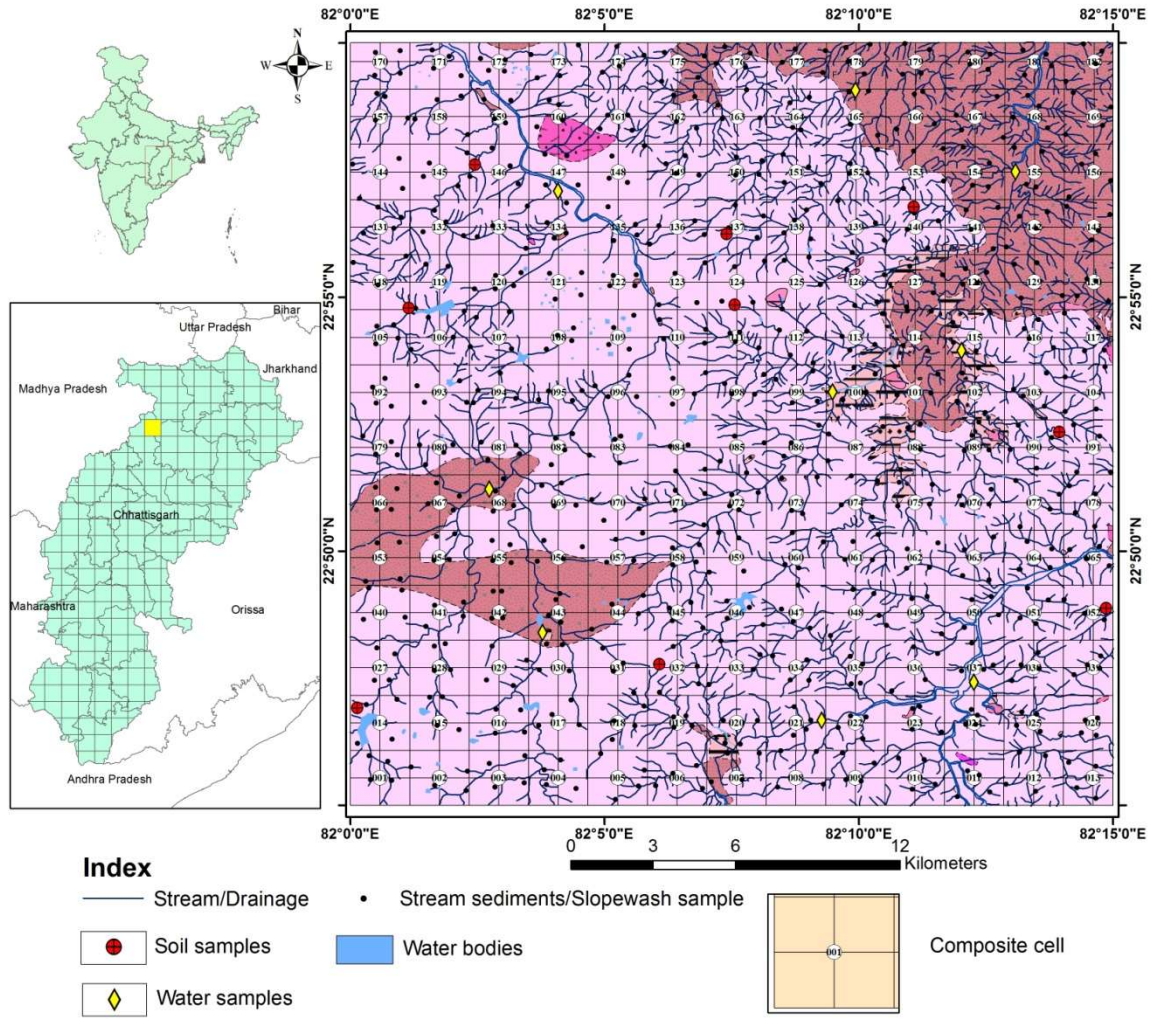

Fig. 1: Gridded geological map showing the location of the study area with stream sediments or slope wash, soil, and water sample location points.

This publication is licensed under a Creative Commons Attribution 4.0 International License

their numerous tributaries, form the main drainage system in the eastern part of the area (Fig 1). The Son River drains the western part of the area. These are non-perennial streams; thus, rainfall is the main recharge source for surface and groundwater. The area receives an average annual rainfall of 1329 mm (CGWB 2013). The rainfall is mostly confined to July and September; the remaining months will be dry. Due to this reason, most of the agricultural activity in the low-lying cultivation areas largely depends upon the surface water sources. These agricultural lands comprised 40 to 50% of the present-day land use pattern in the area, as shown in Fig. 2. The remaining portions are occupied by forest cover (62%) and settlements and water bodies (6%).

The main objective of the present study is to assess the concentrations of heavy metals in the stream sediments and surface water bodies located in the study area, depth-wise geochemical characteristics and distribution of heavy metals in the soil profile, and finally, to assess the irrigation water quality of the surface water bodies present in the area.

GEOLOGICAL SETTING

The area mainly forms part of the central Indian peninsular shield, exposes rocks of the Chhotanagpur gneissic complex, metasediments of the Bilaspur-Raigarh-Surguja Belt, and sedimentary sequences of the Lower Gondwana Group. Chhotanagpur gneissic complex (Peninsular Gneiss) of Archaean-Proterozoic age forms the basement in this area. This mainly consists of granite gneiss with its variant biotite gneiss, grey biotite hornblende gneiss, and porphyritic granite gneiss containing amphibolite enclaves. Granite gneiss are medium to coarse-grained, consisting of quartz, feldspar, and biotite, and are generally foliated. These rocks are traversed by basic dykes, pegmatite, and quartz veins. These gneisses are intruded by granite of various textural, mineralogical characters, such as massive porphyritic to coarse-grained and pink to grey. Granite is the most predominant rock type in the area. It is generally medium to coarse-grained, pink and grey, and composed essentially of quartz, potash feldspar, sodic plagioclase, and subordinate biotite. High muscovite-rich

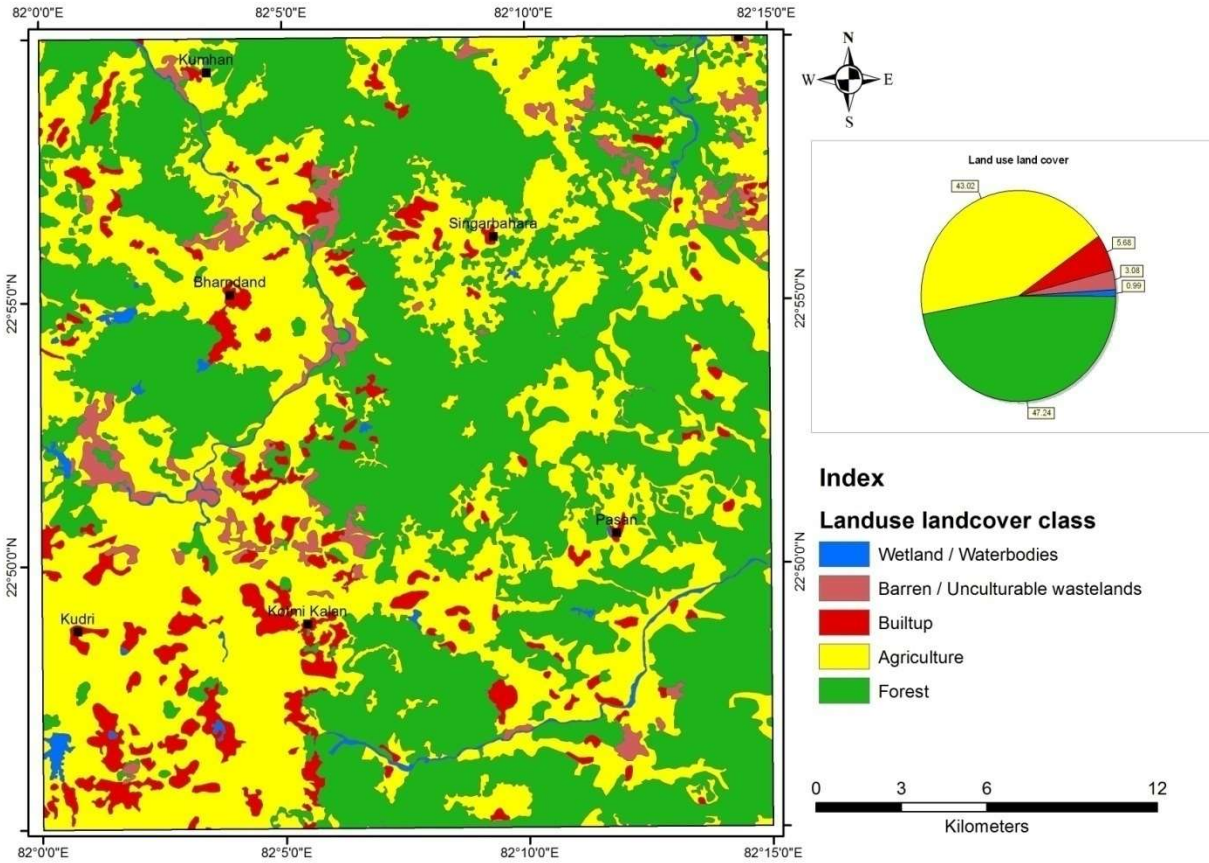

Fig. 2: Land-use land cover map of the study area.

This publication is licensed under a Creative Commons Attribution 4.0 International License

granite is found in the southeastern part of the area, mainly south of Pasan. Muscovite, in association with biotite, occurs in granite in the northwestern part of the area.

The Bilaspur Raigarh Surguja belt (BRS) belt of Archaean-lower Proterozoic age overlying the Chotanagpur Gneissic Complex comprises low to medium-grade metasedimentary rocks, mainly phyllite, quartzite, calc gneiss, calc granulite, garnetiferous mica schist, quartz schist, mica schist, talc schist, biotite schist, marble, and amphibolite. Phyllite is fine-grained, buff, khaki green to green in color with distinct phyllitic sheen. In association with quartz chlorite-schist and quartzite, the phyllite is

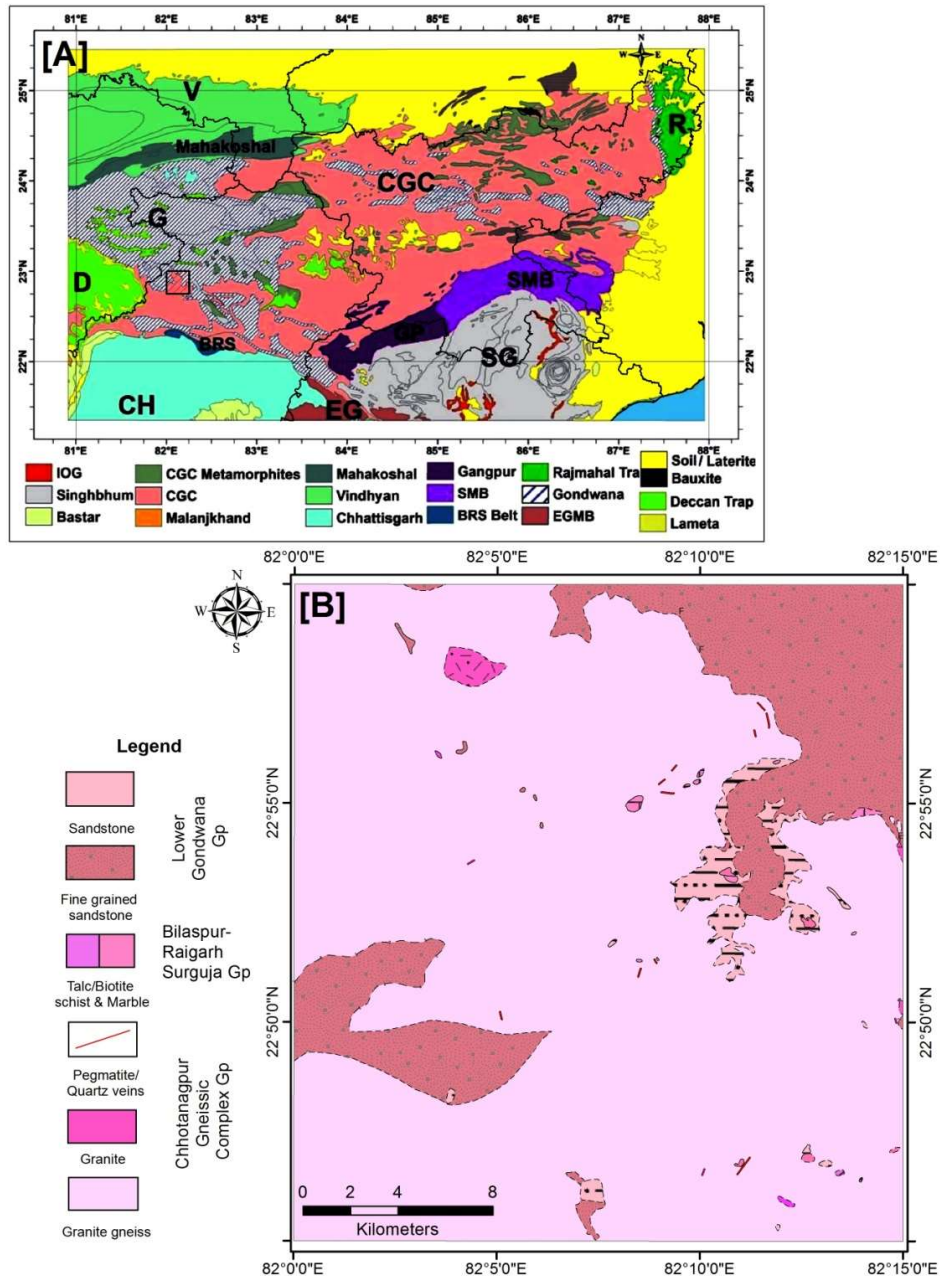

Fig. 3: (A) Regional geological map of Chotanagpur Granite Gneissic Complex (modified after Archaryya 2003, Maji et al. 2008) and (B) geological map of the area in toposheet no 64J/01 in parts of Bilaspur and Korba districts of Chhattisgarh.

This publication is licensed under a Creative Commons Attribution 4.0 International License

seen gradually grading into biotite-gneiss. Quartz schist is fine to medium-grained, purple, and massive to schistose. Garnetiferous mica schists are greyish green to Khakhi grey in color and fine-grained with porphyroblasts of garnet. The mica schist is a fine to medium-grained, well-foliated rock comprising biotite, muscovite, quartz, and feldspars. Talc schist is greenish and fine-grained with a splintery character. The major mineral constituents are actinolite, tremolite, quartz, and plagioclase. Biotite schist consists essentially of quartz and biotite. Iron oxide and plagioclase occur as accessories. The marble is hard, compact, and massive, showing color and grain size variation. The marble is mostly serpentinised and contains tremolite needles in places. Amphilbolites are coarse-grained, dark grey, massive, hard, and non-foliated. The rock comprises hornblende, plagioclase, quartz, biotite, zircon, and opaques.

Talchir Formation of the Lower Gondwana Group tops the whole sequence. The rocks of Talchir formations exposed in the area are mainly conglomeratic bed, shale, and fine-grained sandstone units. It is observed in the northeastern portion of the area. The shales, at places, overlie directly on the granite of the Archean age. The shales are friable and purple, greenish grey and grey. Multiple joints traverse it. These joints have produced the feature of needle shale, where the rock has broken along joints into thin pencil-like prismatic fragments. At places, shales are interbedded with calcareous shale bands, usually less than 15 cm in thickness. The shales are overlain by sandstone. In places, sandstone is directly lying over the Archaean as an overlap. The sandstone is friable, fine to medium-grained, and is composed of quartz and feldspar. It is green, greenish yellow. Fig 3. B shows the detailed geological map of the area.

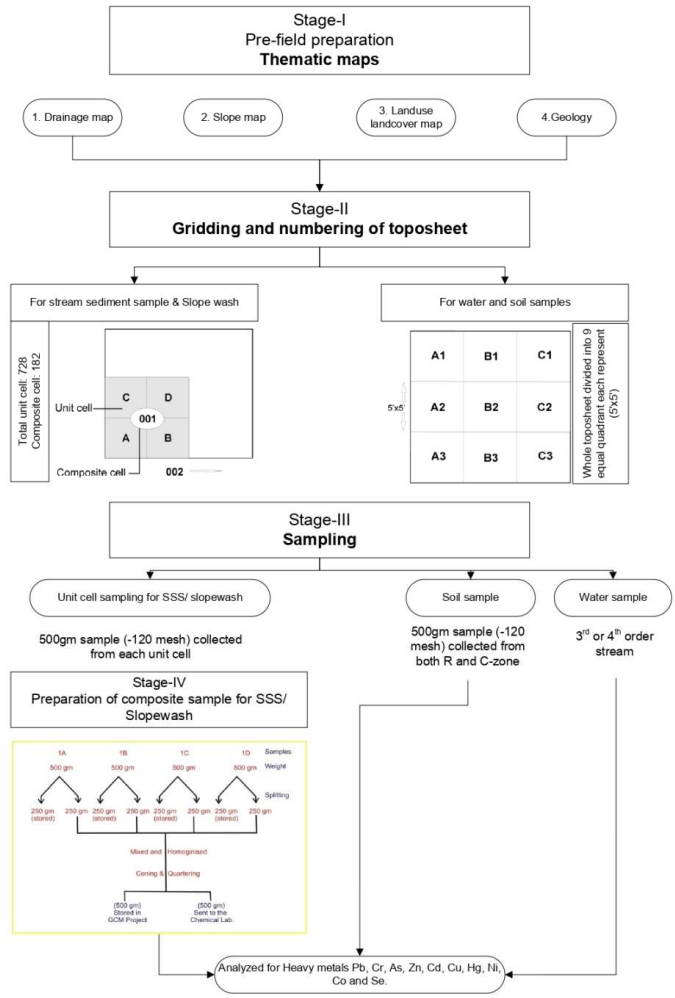

Fig. 4: Methodology flowchart showing different stages involved in geochemical mapping.

This publication is licensed under a Creative Commons Attribution 4.0 International License

MATERIALS AND METHODS

The methodology adopted to achieve the research objective begins with the preparation of different thematic maps such as a drainage map, slope, land-use land cover map, and detailed study of the area's geology. The drainage map on a 1:50,000 scale is divided into a small grid cell called the unit cell, each representing about 1 sq. km area, and tentative sample location points are placed in each small grid. It has been followed by collections of samples from each sq. km area in case of stream sediments and slope wash. For soil and water samples, the 728 sq. km area of the whole toposheet has been divided into 9 large squares having dimensions 9 km x 9 km, and samples have been collected from each of the 9 quadrants. The flow chart of the methodology followed has been illustrated in Fig. 4.

Sampling and Preparation

Samples from different sampling media such as stream sediments/slope wash, regolith (R), and C-horizon of soil and stream water represent the most surface environment. For regional surveys, drainage sediment samples are an appropriate evaluation medium because they more accurately reflect the chemistry of a much larger area than soil samples (Appleton & Ridgway 1992). For the collection of stream sediment samples, the existing drainage in the toposheet 64J/01 has been digitized in a GIS environment and then divided in a 1 kmx1 km cell grid (Fig. 1). A total of 728 nos. of samples has been collected from each grid which will represent an area of 1 sq. km. Samples were collected from each grid from the 1st and 2nd order channels. As these lower-order river-lets are non-perennial, most of the streams in plain areas don't have any water in flowing conditions, mainly during the post-monsoon season from September to March. Hence, most of the lower-order drainage in the area has been modified to agricultural land by the locals. At places where the streams are absent, samples have been collected from the slope wash based on the existing terrain gradient, representing the one sq. km area. Samples from four adjacent 1 km × 1 km cells have been mixed and homogenized through conning and quartering to make one composite sample (NGCM SOP 2011). 182 nos. of such composite samples were analyzed for heavy metal concentration in the area. Sample location points in the gridded drainage map superimposed on the geological map of the study area are shown in Fig. 1.

To assess the variation in heavy metal concentration in the uppermost layer of the earth's crust and to see its vertical distribution, soil samples have been collected from 9 different sites, each representing a grid of 9 × 9 km. In the vertical soil profile, samples have been collected from the topsoil/upper horizon (5-50 cm), referred to as Regolith (R), avoiding the top organic layer (0-5 cm). Samples are also being collected from the bottom C-horizon within a 50-200 cm depth range in each location. Comparison of a C-soil and regolith would give information about elemental behavior in weathering or pedogenic processes, environmental changes affecting the layers, and anthropogenic contamination of the top layer (R). Water sampling is done within the study area to study the interplay between the geosphere and hydrosphere. Nine water samples have been collected, representing the surface water quality. The surface water bodies in the area are the primary source of agricultural water available and are also occasionally used as drinking water in the area, directly affecting human health.

Each stream sediment/slope wash sample and the soil R- and C samples have been sun-dried, de-lumped with a wooden mortar and pestle, and finally sieved through 120 mesh size using a standard stainless steel sieve of ASTM standard. The sample was then conning and quartered, and 250 g samples were selected after homogenization following NGCM SOP 2011. These samples have been analyzed for heavy metal concentration through different analytical techniques.

All the samples were analyzed in the Geological Survey of India's laboratory at Chemical Division, Central Region, Nagpur, India. For stream sediments and soil samples, the heavy metals considered for the present investigation include Co, Cr, Cu, Ni, Pb, Zn, and Se, which are analyzed through XRF techniques; As through HG-AAS; Cd and Ag through GS-AAS and Hg through CV-AAS.

Stream Sediment Samples and Analysis

The analytical results of heavy metals observed in the stream sediment samples were analyzed using basic statistics and spatial distribution maps. The elements considered for the present investigation are Pb, Cr, As, Zn, Cd, Cu, Hg, Ni, Co, and Se. Statistical methods were applied to comprehensively understand the elemental data set's concentrations, deviation, and distribution. The basic statistical parameters determined include mean, standard error, median, mode, standard deviation, sample variance, kurtosis, skewness, range, minimum, maximum, and count. Histograms for each element were also prepared to visualize the data distribution pattern and check for outliers. Elemental distribution maps are prepared using ArcGIS software, and the distribution pattern of each element represented by the contours is overlapped on the geological map of the area so that the anomaly zones can be easily interpreted in terms of the lithology.

Soil Samples Analyses

A total of nine nos. of samples were collected from the area

This publication is licensed under a Creative Commons Attribution 4.0 International License

such that each sample represents an area of 81 sq km so that a detailed representation of the nature and type of soil can be made. Two samples were taken from each location, one from the topsoil or Regolith/R-horizon (after removing the organic layer) and another from the bottom C-horizon. Both samples were analyzed for selective heavy metal concentrate as in the sediments/slope-wash sample case.

Water Sample Analyses

Water samples have been collected from flowing streams to represent the elemental distribution of that particular drainage basin. 9 samples have been collected from the study area, as shown in Fig 1. Field measurements, including temperature (°C), electrical conductivity (EC), total dissolved solids (TDH), and pH, were carried out using standard field equipment. For IC ion analysis, five hundred milliliters of water samples were collected in a polyethylene bottle. The bottle was rinsed with sample water twice before filling it up by submerging it completely under water so that no air bubbles were left. Once the bottle is full, it has been closely tight below the water level.

To determine other heavy metals and trace elements through ICP-MS and ICP-AES analysis, another 100 mL filtered water sample was collected, and soon after collection, 1.0 mL of conc. HNO_3 has been added through a droplet bottle. The tightly closed bottle was shaken to mix the acid well with the sample water. TDS in the irrigation water was measured by weighting, the concentration of Cl^- was measured by the colorimetric methods using a micro flux auto analyzer, the content of SO_4^{2-} was determined by volume, the concentrations of Mg^{2+}, and Ca^{2+} were dignified by the AAS, and the contents of K^+, Na^+ were determined by the flame emission spectroscopy, HCO_3^-, CO_3^{2-}. Alkalinity was determined by the acid titration method (NGCM SOP 2011).

The suitability of irrigation water was assessed using sodium adsorption ratio (Richards 1954), sodium percentage (Wilcox 1955), residual sodium bi-carbonate (Gupta & Gupta 1987), permeability index (Doneen 1964), magnesium hazard ratio (Paliwal 1972) and Kelley's ratio (Kelly 1963). They were computed using the following equations:

$$\text{Sodium Adsorption Ration (SAR)} = \frac{Na^+}{\sqrt{\frac{(Ca^{2+}+Mg^{2+})}{2}}} \quad \ldots(1)$$

$$\text{Sodium percentage (Na\%)} = \frac{(Na^+ + K^+)\times 100}{(Ca^{2+}+Mg^{2+}+Na^+ + K^+)} \quad \ldots(2)$$

$$\text{Residual sodium bi} - \text{carbonate (RSBC)} = HCO3^- + Ca^{2+} \quad \ldots(3)$$

$$\text{Permeability index (PI)} = \frac{Na^+ + \sqrt{HCO3^-}}{Ca^{2+}+Mg^{2+}+Na^+} \times 100 \quad \ldots(4)$$

$$\text{Magnesium hazard (MH)} = \frac{Mg^{2+}}{Ca^{2+}+Mg^{2+}} \times 100 \quad \ldots(5)$$

$$\text{Kelly index (KI)} = \frac{Na^+}{Ca^{2+}+Mg^{2+}} \quad \ldots(6)$$

Where all ion concentrations are expressed in meq/L.

RESULTS AND DISCUSSION

The details of the heavy metal concentrations observed in stream sediments and slope wash samples from the area are given in Table 1, with all the statistical parameters measured. The concentrations of heavy metals like Pb, Zn, Cu, and Co in stream sediments/slope-wash samples are observed to be higher than their upper continental crust (UCC) abundance. Other elements like Cr, Cd, Hg, Ni, and Se concentrations are below UCC value. Almost all the element's distributions are positively skewed, and apart from Cr, Ni, and Co, all have positive kurtosis. When compared with the globally acceptable permissible or critical limits of each element, it has been observed that the concentration of Pb, Cd, Cu, Hg, and Se is well within safe limits. Slightly higher concentrations are observed in Cr, As, Zn, and Co but not higher than the critical range. The Ni concentration in the area shows maximum values of 47.0 ppm, mainly in the southwestern part, and falls under a slight contamination range as per Alloway 1990.

The elemental distribution map for Ni has been superimposed over the geological map of the area (Fig. 5.viii) to observe any geogenic causes for these higher concentrations. Higher values of Ni with anomaly are present in and around Bharidand and south of Kodri village. The area is occupied by mainly granite gneiss of the Chhotanagpur Gneissic Complex. Cr values also show a slightly high concentration in these areas, mainly in the western part (Fig. 5.ii). High 'As' concentrations are observed in the southwestern part near Kudri village, similar to Ni (Fig. 5.iii). Similarly, Higher values of Cr with anomaly are present mainly north of Kodri and east of Bhaarridand village, where the litho unit is Granite gneiss of the CGC group. At the same time, Zn and Co show high concentration in Singarbahar, south of Kotmikalan, and near Pasan villages occupied by Granite gneiss (Fig. 5.iv & 5.ix).

This publication is licensed under a Creative Commons Attribution 4.0 International License

Table 1: Values of statistical parameters calculated for different heavy metals (in ppm) in stream sediment samples and their permissible limits in soil.

Elements	Statistical parameters							Permissible limits	Reference
	Maximum	Minimum	Mean	Skewness	Kurtosis	Threshold value	UCC abundance		
Pb	77.00	22.00	35.54	1.33	2.67	53.26	17.00	250-500	Awasthi 2000
Cr	78.00	10.00	28.15	0.78	-0.4	63.38	92.00	1-100	Alloway 1990
As	11.21	1.00	4.50	0.72	0.28	9.09	9.00	0-30	Alloway 1990
Zn	248.00	35.00	15.15	1.95	5.39	122.41	67.00	150-300	Mushtaq & Khan 2010
Cd	0.137	<0.1	0.053	4.38	18.03	0.08	0.09	1.0-3.0	Mushtaq & Khan 2010
Cu	70.00	6.00	18.90	2.16	11.82	33.75	28.00	135-270	Awasthi 2000
Hg	0.037	<0.005	0.012	1.26	1.10	0.026	0.05	0-1	Alloway 1990
Ni	47.00	5.00	20.71	0.73	-0.01	38.57	47.00	0-20	Alloway 1990
Co	26.00	8.00	15.28	0.30	-0.46	23.07	17.30	1.0-40.0	Alloway 1990
Se	0.82	0.10	0.30	0.61	0.75	-0.02	0.90	0-1	Alloway 1990

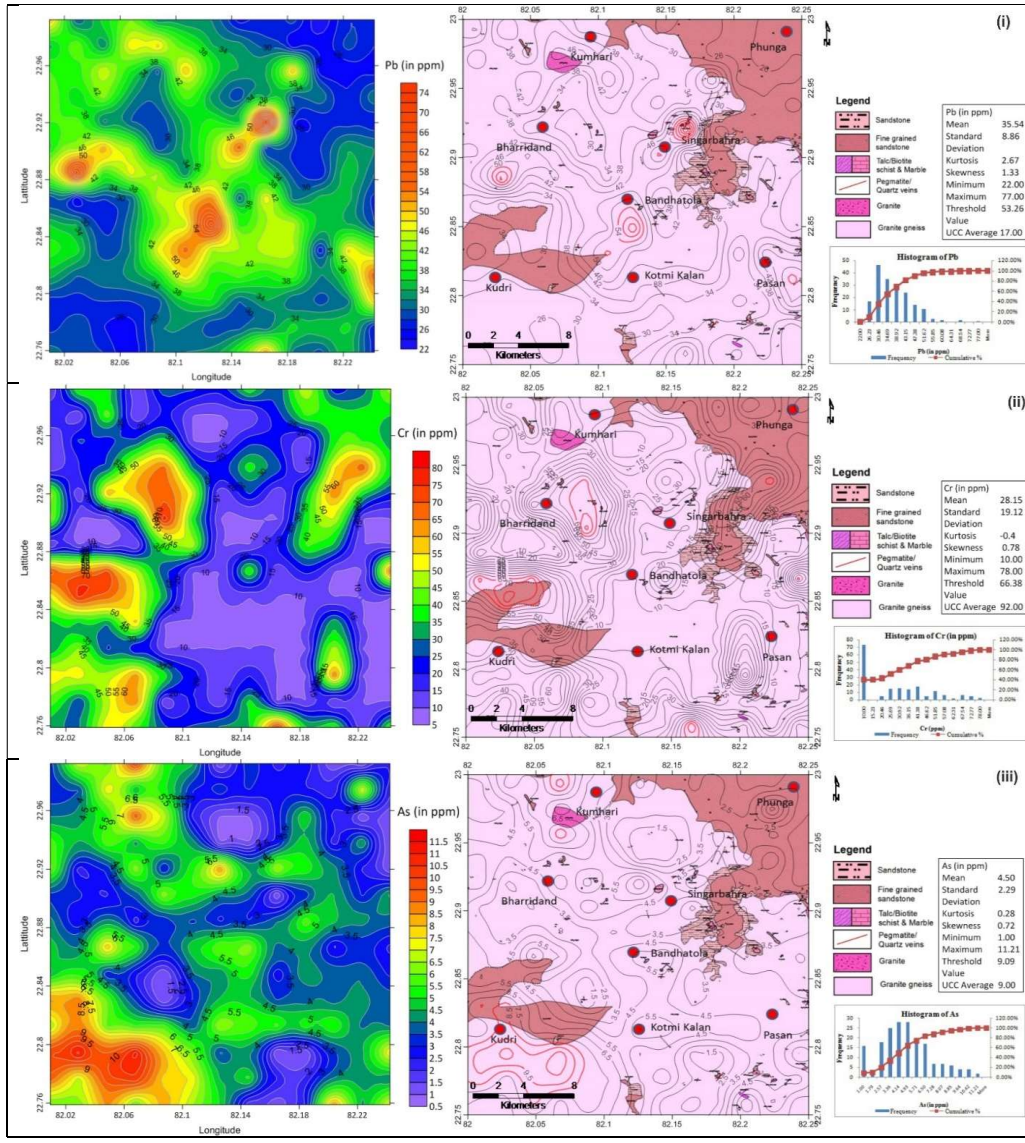

Figure Cont....

This publication is licensed under a Creative Commons Attribution 4.0 International License

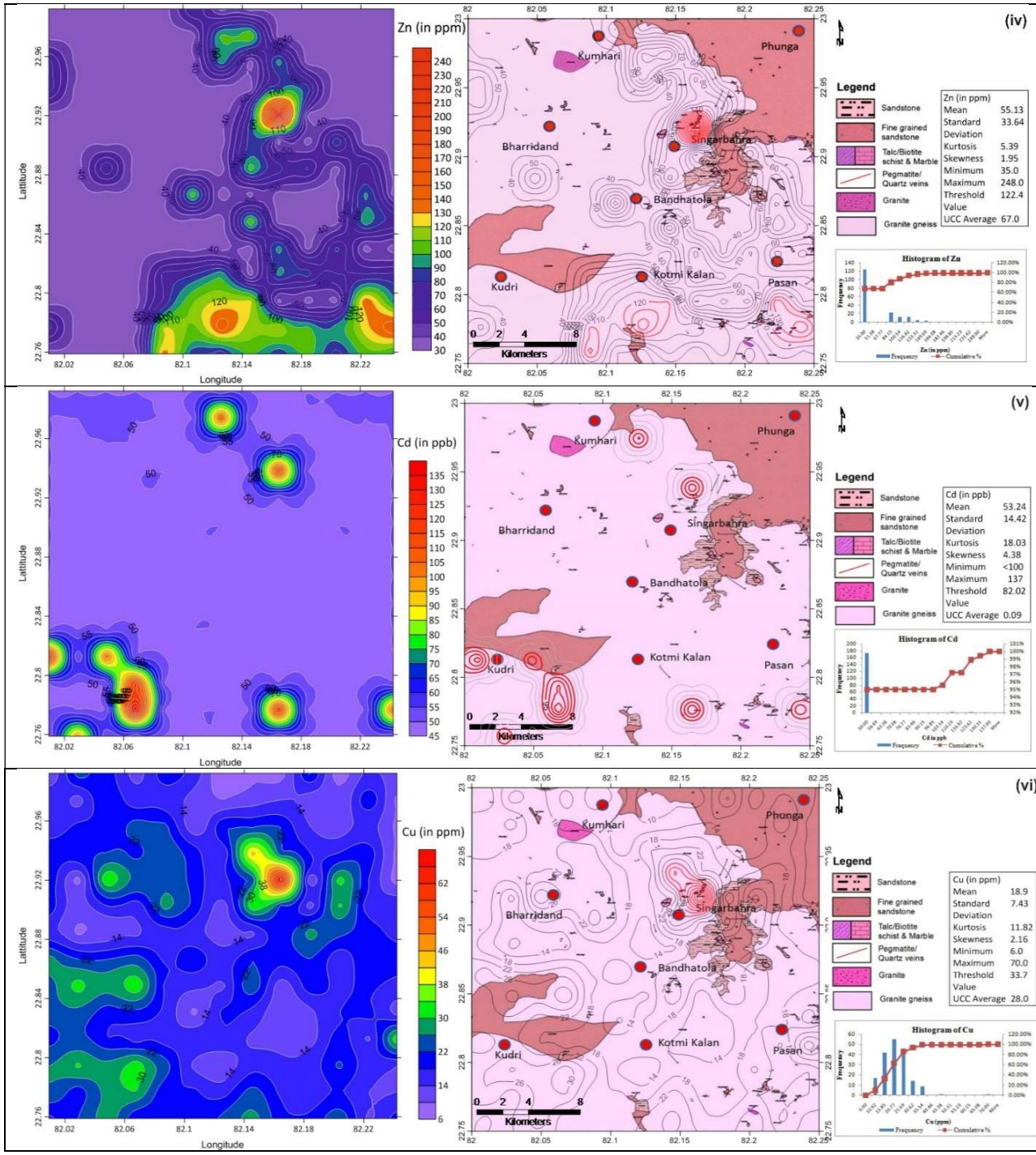

Figure Cont....

This publication is licensed under a Creative Commons Attribution 4.0 International License

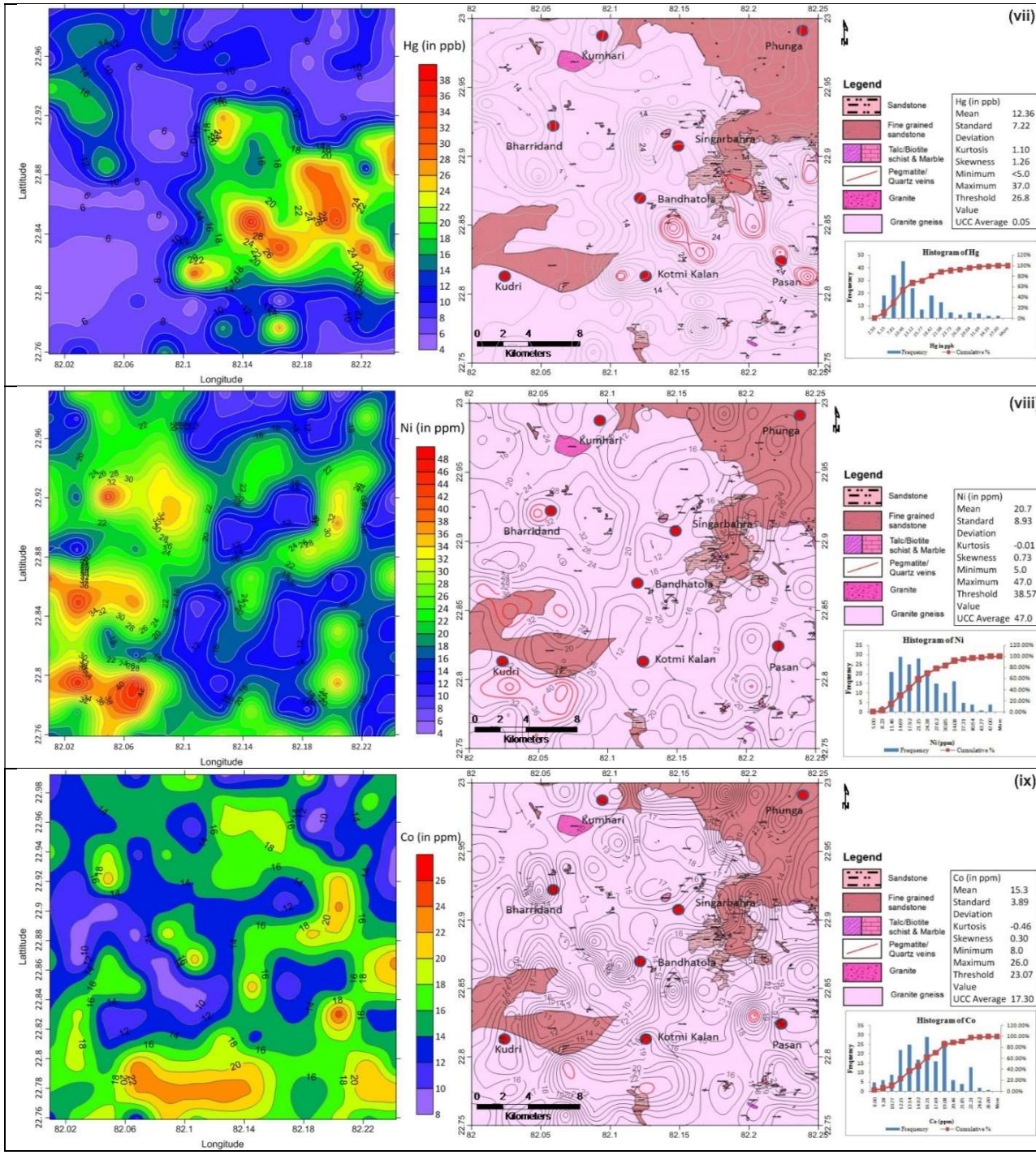

Figure Cont....

This publication is licensed under a Creative Commons Attribution 4.0 International License

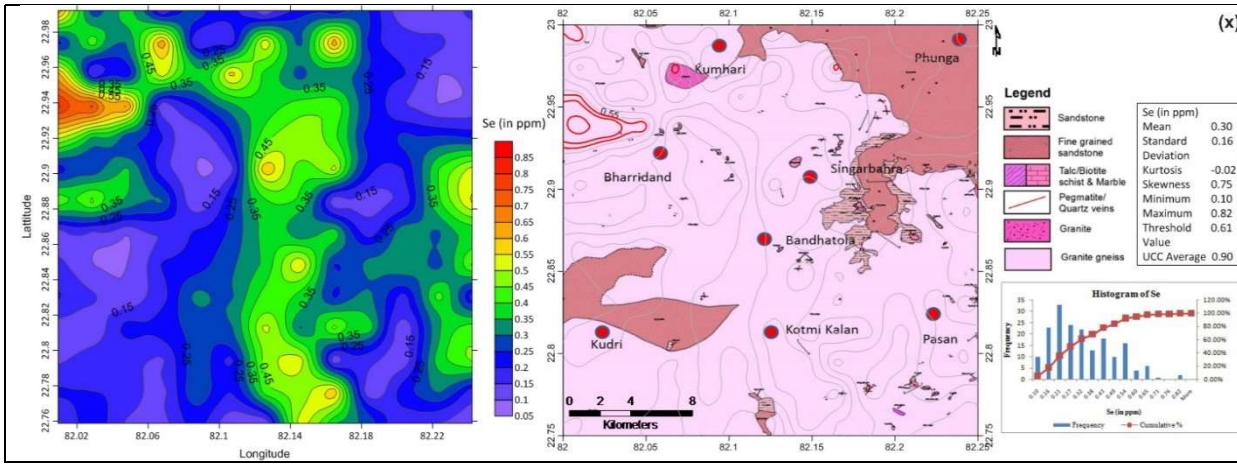

Fig. 5: Geochemical distribution map of heavy metals in stream sediments/slope wash samples in the area and contour diagram superimposed on the geological map of T.S. no 64J/01 for i. lead (Pb), ii. Chromium (Cr), iii. Arsenic (As), iv. Zinc (Zn), v. Cadmium (Cd), vi. Copper (Cu), vii. Mercury (Hg), viii. Nickel (Ni), ix. Cobalt (Co) and x. Selenium (Se).

The remaining heavy metals occur as minor concentrations in the area are Pb, within the granite gneiss of Chhotanagpur Gneissic Complex in the area mainly near Singarbahra and south of Bharridand village (Fig. 5.i). The abnormal value of Cd are observed in the north-east of Singarbahra and Bharridand village. The lithology of this area is mainly Granite Gneisss of the Chotanagpur Gneissic Complex (Fig. 5.v). Higher values of Cu are present in and around Singarbahra village, occupied by granite gneiss of the CGC group (Fig. 5.vi). The highly concentrated anomaly of Hg is observed in the southeast of Singarbahra, Bandhatola, and Pasan villages over Granite Gneisss of Chotanagpur Gneissic Complex and sandstone rocks of Lower Gondwana group (Fig. 5.vii). A highly concentrated anomaly for Se is observed northwest of Bharridand village, in the granite gneiss of Chhotanagpur Gneissic Complex (Fig. 5.x).

The vertical distribution of heavy metal concentrations in the area has been assessed through several soil samples from R- and C-horizon. Analytical results for nine such samples were shown graphically in Fig. 6. 'Pb' ranges from 26 to 46 ppm in the area where samples from the central portion of the area show high concentration. 'Cr' ranges from 15 to 87 ppm in R-horizon and 15 to 77 ppm in C-horizon. 'As' concentration in soil samples varies from 2.56 to 13.22 ppm in the R-horizon and 2.87 to 6.93 ppm in the C-horizon. 'Zn' concentration ranges from 60 to 107 ppm in both R and C- horizons. The 'Cd' value in the R-horizon is <100 ppb, whereas the maximum value of Cd is observed to be 147 ppb in the C-horizon. 'Cu' ranges from 8 to 34 ppm in the R-horizon, whereas in C-horizon, Cu ranges from 10 to 38 ppm. 'Hg' concentration ranges from 2.5 to 15 ppb and 7 to 17 ppb in the R- and C- horizons, respectively. 'Ni' values range from 14 to 51 ppm in R-horizon and 14 to 61 ppm in C-horizon. 'Co' values range from 9 to 24 ppm and 5 to 25 ppm in R- and C-horizon, respectively, whereas the Se concentration in R-horizon ranges from 0.1 to 0.5 ppm and 0.2 to 0.75 ppm in C-horizon.

Fig 6 shows that almost all heavy metal concentrations are higher in the bottom C-horizon than in the top regolith zone, except for 'Zn' in samples no SS-06, 08, and 09. High-density heavy metals concentrate at the bottom of the soil profile, thus increasing the concentration in the C-horizon. A high Zn value in the R-horizon at the southeastern part of the area is mainly due to anthropogenic changes such as higher uses of fertilizer in agricultural lands. Higher values of Ni and Cr have also been observed in sample no SS-03, from the southwestern part where Ni: 31 ppm and 54 ppm and Cr: 64 ppm and 87 ppm in R and C-samples, respectively.

Higher concentrations of Ni-Cr are mainly seen in the area occupied by mafic or ultra-mafic rocks (Alloway 1990). Nickel is relatively more abundant than chromium and widely distributed in the earth's crust. Nickel concentrations in the soil largely depend on the parent rocks. The lowest contents are found in sedimentary rocks comprising clays, limestones, sandstones, and shales, while the highest concentrations exist in basic igneous rocks (Kabata-Pendias & Mukherjee 2007). Ultramafic rocks such as peridotite, dunite, and pyroxenite have the highest Ni concentrations, followed by mafic and intermediate rocks. However, in surface soils, its content also reflects pedogenic processes and pollution (Kabata-Pendias & Pendias 1992). In the present area of investigation, no such mafic or ultramafic bodies were observed, as shown in the lithological map of TS no 64J/01 (Fig. 3. B). The higher concentrations of Ni and Cr are mainly observed in

This publication is licensed under a Creative Commons Attribution 4.0 International License

Fig. 6: Heavy metal concentration in soil (both R- and C- horizon) samples collected from the study area.

the southwestern part of the area occupied by granitoid and granite gneisses (Fig 5. ii & viii). The concentration of Cr and Ni in granitic igneous rocks ranges from 2 to 90 mg kg^{-1} for Cr and 2–20 mg kg^{-1} for Ni (Krishna et al. 2011). The higher concentrations of Ni in stream sediments and soil mightn't be related to any geo-genic source but rather anthropogenic interference. Anthropogenic sources such as industrial waste materials, lime, fertilizer, and sewage sludge constitute the major sources of Nickel in soils (Mcllveen & Negusanti 1994, Chauhan et al. 2008, Iyaka 2011). The study area is mainly a rural-based agroecosystem with no industries or major townships. Therefore, the influence of industrial waste and sewage sludge is very negligible. Phosphate fertilizers are among the sources of heavy metal inputs to agricultural systems (Ramadan & Al-Ashkar 2007). The primary source of fertilizer-derived heavy metals in soils is phosphatic fertilizers manufactured from the phosphate rocks that contain various metals as minor constituents in the ores. Some fertilizers and soil amendments used in agriculture are important sources of Ni in soil. Rock phosphate, which is

This publication is licensed under a Creative Commons Attribution 4.0 International License

used as a raw material for phosphatic fertilizers, is known to contain Ni ranging between 16.8 to 50.4 ppm, and other fertilizers like ammonium nitrate (<0.20 ppm) and triple super phosphate may also contain 15.6 to 25.2 ppm Ni (Raven & Loeppert 1997).

A few important observations can also be made from the land-use land cover map in Fig 2, where the southwestern part comprises active agricultural activity, villages, and other build-up areas. This area has the highest concentrations of heavy metals like Ni, Cr & As, etc., suggesting the anthropogenic influence mainly from the fertilizer source. Higher concentrations of 'As' are observed in stream sediments, mainly in the southwestern part, similar to Nickel. Whereas higher values of Zn are observed in the southern and south-eastern parts of the area and almost all soil samples. Higher concentrations of As and Zn can also be ascribed to the extensive use of fertilizer and soil amendments. Rock phosphate contains 16.5-20.5 ppm, and Triple superphosphate contains 15.3-16.2 ppm of As, whereas Zn concentrations vary from 78.8-382 ppm in rock phosphate and 61.3 in triple superphosphate (Raven & Loeppert 1997).

Similarly, poultry and swine manure contain an appreciable amount of Zn in the order 330-456 and 540-1200 ppm, respectively (Wolfgang & Dohler 1995). The other heavy metals like Pb, Cd, Cu, Hg, Co, and Se occurs below the permissible limits and have normal distribution pattern. Their anomalous concentrations are observed mainly over the granite gneiss of CGC. Instead of anthropogenic sources, erosion of granite may be the primary cause of heavy metals in granite-gneiss soils (Baltrenaite & Butkus 2004).

Twelve water quality parameters viz., temperature (T), pH, electrical conductivity (EC), total hardness (TH), total dissolved solids (TDS), sodium (Na^+), potassium (K^+), calcium (Ca^{2+}), magnesium (Mg^{2+}), bicarbonate (HCO_3^-), chlorides (Cl^-), sulfates (SO_4^-) were analyzed for quality of surface water for drinking purpose. Samples were also analyzed for concentration of heavy metals like lead (Pb), chromium (Cr), Arsenic (As), zinc (Zn), cadmium (Cd), copper (Cu), nickel (Ni), Cobalt (Co) and Selenium (Se), etc. The analytical results of all the water samples are given in Table 2.

In the current study, the pH ranges between 7.2 (minimum) to 8.2 (maximum); EC values ranged from 224 $\mu S.cm^{-1}$ to 412 $\mu S.cm^{-1}$. The desirable limit of EC for drinking purposes is 300 $\mu S.cm^{-1}$ (Chaurasia et al. 2021).TDS in the area varies from 112 to 206 $mg.L^{-1}$. The permissible limit of TDS in water is 2000 $mg.L^{-1}$, and the ideal TDS for drinking water is below 500 $mg.L^{-1}$ (Shiow-Mey et al. 2004). Due to the prevalence of sodium compounds in rocks and soils, which are easily dissolved, all surface water contains some sodium. The permissible limit of sodium is 200 $mg.L^{-1}$, and in the current study area, it varies from 21.0 to 40.0 $mg.L^{-1}$. Potassium is common in many rocks. The primary source of potassium in natural freshwater is the weathering of rocks, but the quantities increase in the polluted water due to wastewater disposal. Usually, natural surface waters have less than 5 $mg.L^{-1}$ of potassium (Skowron et al. 2018). The present study area K varies from 1.0 to 2.0 $mg.L^{-1}$ within the permissible limit (12 $mg.L^{-1}$). Hardness is directly correlated with calcium and magnesium. Calcium concentration ranged between 27.0 to 50 $mg.L^{-1}$ and was found below the permissible limit (200 $mg.L^{-1}$). The magnesium content in the investigated water samples ranged from 5 to 14 $mg.L^{-1}$, within the permissible limit (100 $mg.L^{-1}$). The permissible limit of total hardness as $CaCO_3$ is 600 $mg.L^{-1}$ for drinking water. In the current study, hardness ranges from 88 to 156 $mg.L^{-1}$, which is within the permissible. The effects of the carbonate equilibrium typically maintain natural waters' bicarbonate concentrations within a moderate range. Most surface streams had bicarbonate and carbonate concentrations below 200 $mg.L^{-1}$ but in groundwater, somewhat higher (Kumar et al. 2016). Bicarbonate concentration in the surface water samples ranges from 131 to 220 $mg.L^{-1}$, thus within the permissible limit (500 $mg.L^{-1}$) (WHO 2011). The most common natural form of chlorine is chloride, which is incredibly stable in water. The high concentration of chloride is considered to be an indication of pollution due to increased organic animal waste (Comly 1945). The desirable limit and permissible limit for chloride, according to the World Health Organization (WHO 2011) and Bureau of Indian Standards (BIS 1991), are 250 and 1000 $mg.L^{-1}$, respectively. In the present study, the concentration of Cl ranges from 10 to 15 $mg.L^{-1}$, thus within the limit. The sulfate concentration varied between 3 $mg.L^{-1}$ and 22 $mg.L^{-1}$, under the permissible limit (1000 $mg.L^{-1}$).

All the water samples have also been analyzed for heavy metals, and the results show that Pb concentration ranges from <0.5 to 5.4 ppb; Cr ranges from 4.6 to 10.2 ppb; Cu values range from 0.8 to 1.33 ppb; Co value ranges from 0.07 to 0.42 ppb. Heavy metals like As, Zn, Cd, Ni, and Se present below detectable limits in the water samples. All vales are below the permissible limit of drinking water norms as par BIS standards (BIS 1991).

Correlation Analysis

The correlation matrix has been prepared for the fifteen physical and chemical parameters to assess the inter-elemental relationship (Table 3). The correlation coefficient expresses numerically the extent to which two variables are statistically associated. A correlation coefficient

This publication is licensed under a Creative Commons Attribution 4.0 International License

of <0.5 exhibits poor correlation, 0.5 indicates a good correlation, and >0.5 represents excellent correlation (Kumar et al. 2016).

Some significant correlations observed in the correlation matrix are discussed below. The correlation matrix shows that the pH shows moderate to good correlation with almost

Table 2: Analyzed physico-chemical water quality parameters of nine surface water samples collected from the study area.

Sample No.	Temp. (°C)	pH	E.C. ($\mu S.cm^{-1}$)	TDS ($mg.L^{-1}$)	Na^+ ($mg.L^{-1}$)	K^+ (mg/l)	Ca^{2+} ($mg.L^{-1}$)	Mg^{2+} ($mg.L^{-1}$)	T.H. as $CaCO_3$	HCO_3^- ($mg.L^{-1}$)	Cl^-($mg.L^{-1}$l)	SO_4^{2-} (mg/l)	Pb (ppb)	Cr (ppb)	As (ppb)	Zn (ppb)	Cd (ppb)	Cu (ppb)	Ni (ppb)	Co (ppb)	Se (ppb)
64J01/ A1/W/18	16.4	7.3	236	118	21.0	1.0	32.0	7.0	108	131	10	3	5.4	4.6	<1	<2	<0.01	0.9	<1	0.4	<100
64J01/ A2/W/18	18.7	7.9	224	112	21.0	2.0	32.0	5.0	100	131	10	9	3.5	7.3	<1	<2	<0.01	0.9	<1	0.3	<100
64J01/ A3/W/18	18.7	8	242	121	22.0	2.0	29.0	7.0	100	136	11	6	2.9	10.2	<1	<2	<0.01	1.0	<1	0.1	<100
64J01/ B1/W/18	19.7	8.2	330	165	40.0	2.0	27.0	10.0	112	157	13	22	0.6	6.1	<1	<2	<0.01	1.1	<1	0.1	<100
64J01/ B2/W/18	14.8	7.9	412	206	31.0	2.0	50.0	8.0	156	220	15	12	<0.5	5.0	<1	<2	<0.01	1.3	<1	0.1	<100
64J01/ B3/W/18	16.6	7.4	254	127	26.0	2.0	30.0	6.0	100	142	15	7	3.2	7.0	<1	<2	<0.01	1.0	<1	0.3	<100
64J01/ C1/W/18	15.6	7.2	312	156	31.0	1.0	30.0	11.0	124	163	11	13	<0.5	5.0	<1	<2	<0.01	1.1	<1	0.1	<100
64J01/ C2/W/18	19.5	8.2	352	176	30.0	1.0	35.0	14.0	148	199	13	11	<0.5	5.3	<1	<2	<0.01	1.2	<1	0.1	<100
64J01/ C3/W/18	18	7.6	258	129	23.0	1.0	27.0	5.0	88	147	10	4	<0.5	5.2	<1	<2	<0.01	1.3	<1	0.1	<100

Table 3: Correlation matrix between various surface water quality parameters.
The bold values in the correlation matrix show that the element correlated with >0.50.

	pH	E.C.	TDS	Na^+	K^+	Ca^{2+}	Mg^{2+}	Total hardness	HCO_3^-	Cl^-	SO_4^{2-}	Pb	Cr	Cu	Co
pH	1														
E.C.	0.37	1													
TDS	0.37	1.00	1												
Na^+	0.37	**0.74**	**0.74**	1											
K^+	0.42	0.02	0.02	0.15	1										
Ca^{2+}	0.17	**0.70**	**0.70**	0.12	0.19	1									
Mg^{2+}	0.31	**0.64**	**0.64**	**0.64**	-0.36	0.14	1								
Total hardness	0.30	**0.89**	**0.89**	**0.50**	-0.08	**0.80**	**0.71**	1							
HCO_3^-	0.36	**0.96**	**0.96**	**0.55**	-0.05	**0.78**	**0.60**	**0.93**	1						
Cl^-	0.24	**0.65**	**0.65**	**0.55**	0.46	**0.52**	0.28	**0.55**	**0.63**	1					
SO_4^{2-}	0.48	**0.61**	**0.61**	**0.93**	0.31	0.07	**0.55**	0.41	0.40	0.41	1				
Pb	-0.35	-0.73	-0.73	-0.69	0.12	-0.18	-0.52	-0.46	-0.68	-0.33	-0.58	1			
Cr	0.34	-0.45	-0.45	-0.31	**0.62**	-0.29	-0.31	-0.42	-0.43	-0.06	-0.13	0.29	1		
Cu	0.19	**0.62**	**0.62**	0.34	-0.24	0.32	0.21	0.36	**0.66**	0.35	0.10	-0.80	-0.37	1	
Co	-0.49	-0.66	-0.66	-0.63	0.02	-0.15	-0.54	-0.44	-0.60	-0.18	-0.61	0.92	0.03	-0.63	1

This publication is licensed under a Creative Commons Attribution 4.0 International License

all parameters while negatively correlated with lead and cobalt. Electrical conductivity and total hardness (TDS) show a positive correlation with most of the parameters except with heavy metals like lead (-0.73), Cr (-0.45), and cobalt (-0.66). Sodium exhibits a poor positive correlation with potassium (0.15). A strong positive correlation between sodium and potassium indicates a geogenic source and suggests that sodium and potassium have been derived from the disintegration of silicate minerals (Hem 1991). As there is a poor correlation between sodium and potassium, it can be suggested that the source of sodium may not be geogenic but anthropogenic. Sodium strongly correlates with sulfate (0.93) but moderately with chloride (0.55). This suggests that the source of sodium may be sulfate compounds instead of chlorides. Mirabilite, associated with gypsum, halite, etc., is a geogenic source of sodium sulfate compounds (Wells 1923, Khalili & Torabi 2003).

Moreover, while exposed, pyrite and other sulfides associated with granite and granite gneisses are oxidized to sulphuric acid. This sulphuric acid immediately dissolves some basic oxides, producing soluble sulfates (Wells 1923). As in the study area, no such mineralized sulfide zones were observed during mapping, nor were any reported occurrences of gypsum or halite in the area, so the source of sodium may be anthropogenic. Calcium and magnesium show a strong positive correlation (0.93) and moderate positive correlation (0.60), respectively, with bicarbonates indicating that calcium and magnesium have been derived from the dissolution of carbonate minerals. As the pH of the stream water ranges between 7-8, the carbonate ions formed due to the disassociation of the carbonate minerals are present in the stream water as bicarbonates (Fetter 2001).

Amongst the heavy metals, lead is negatively correlated with almost all parameters. A strong positive correlation is observed between Cr with K (0.62) and Co with Cr (0.90), while both Cr and Co show a negative correlation with rest.

Water Quality Characteristics for Irrigation Purposes

To understand the relationship of the chemical components of water, data was plotted in Gibbs diagram (1970). Three fields of the Gibbs diagram, precipitation dominance, evaporation dominance, and rock-water interaction dominance, are used to determine the quality attributes of water (Kumar et al. 2016), where all ions are expressed in meq.L^{-1}.

$$\text{Gibbs ratio I (for anion)} = \frac{Cl^-}{(Cl^- + HCO_3^-)} \quad \ldots(7)$$

$$\text{Gibbs ratio II (for cation)} = \frac{Na^+}{(Na^+ + Ca^{2+})} \quad \ldots(8)$$

The Gibbs ratio of the water samples is plotted against their respective total dissolved solid concentration (TDS), as shown in Fig. 7. According to Gibbs equations I and II, all the surface water samples fall under the evaporation dominance field. It indicates that evaporation-sedimentation

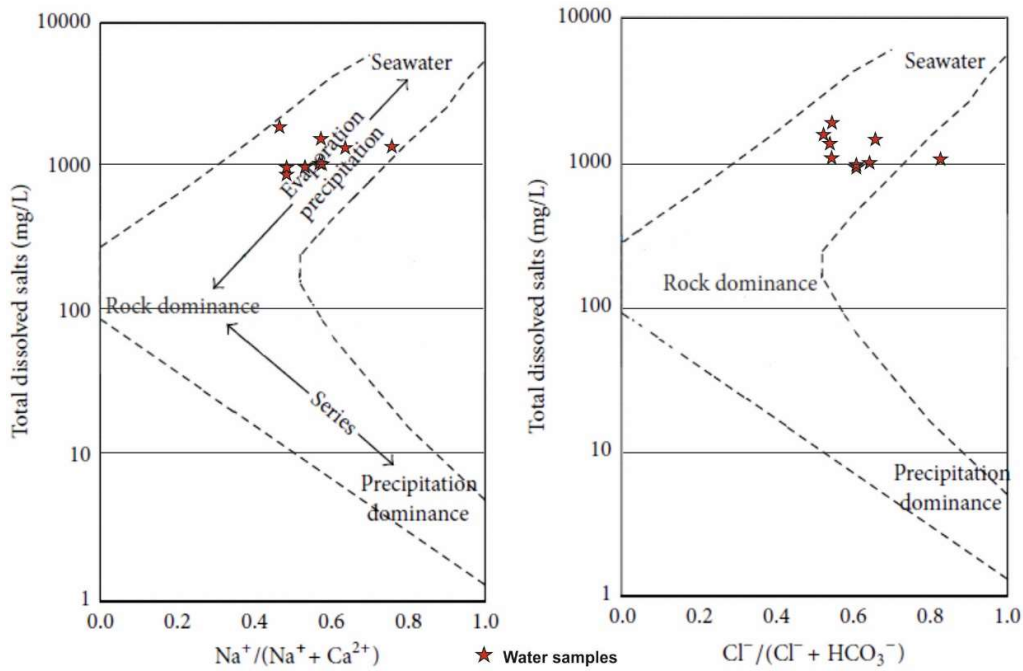

Fig. 7: Gibbs diagram illustrating the mechanism controlling the surface water chemistry.

This publication is licensed under a Creative Commons Attribution 4.0 International License

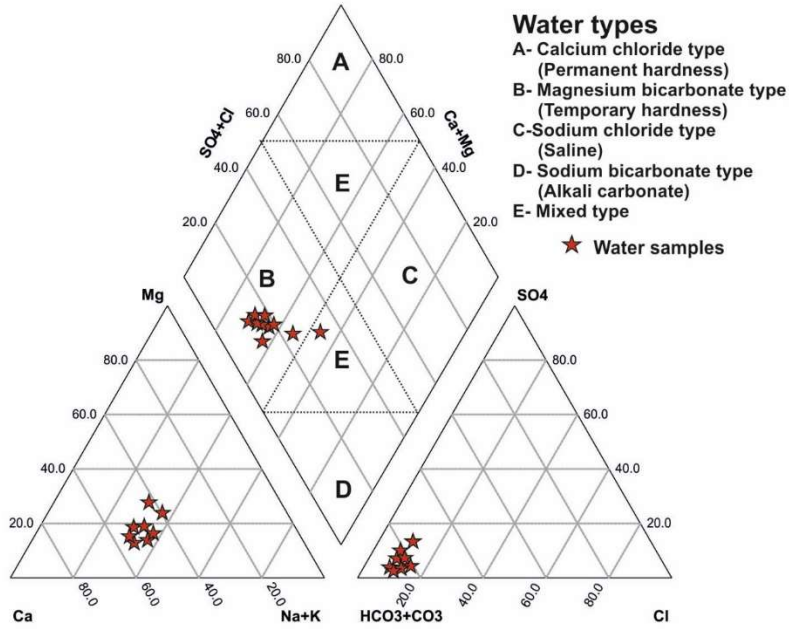

Fig. 8: Piper diagram showing water type in the study area (after Piper 1944).

is the main factor in the chemical composition of surface water bodies. Thus, the chemical weathering of rock-forming minerals doesn't control the surface water chemistry of the study area.

The groundwater type was characterized using the Piper trilinear diagram (1944) and is given in Fig. 8. This diagram shows five zones (Zone A, B, C, D & E). In zones A, B, C, and D, two groups of anions and cations dominate. For example, SO_4^{2-}- Cl^- anions and Ca^{2+}- Mg^{2+} cations dominate in zone A, HCO3 - CO32- anions and Ca2+- Mg2+ cations dominate in zone B, etc. Zone E represents a mixing zone where neither anions nor cations are dominant. The diagram shows that most of the water samples are magnesium bicarbonate type, having temporary hardness.

The sodium hazard of irrigation water was definite by the relative proportion of sodium (Na+) to calcium (Ca^{2+}) and magnesium (Mg^{2+}) ions and was expressed in terms of SAR (sodium absorption ratio). High sodium concentration in water leads to the degradation of soil structure by reducing soil permeability, thus affecting the physical property of soil when used for irrigation purposes (Dhirendra et al. 2009). The SAR values are determined using Eq. 1 (Richards 1954) and varied from 0.88 to 1.67 (Table 4). SAR values >10 were not recommendable for water to be used for irrigation purposes (Siamak & Srikantaswamy 2009). In the present

Table 4: Statistical representation of irrigation water parameters.

Sample No.	SAR	Na%	RSBC	PI	MH	KI
64J01/A1/W/18	0.88	30.17	0.55	77.07	26.51	0.42
64J01/A2/W/18	0.91	32.45	0.55	81.41	20.49	0.45
64J01/A3/W/18	0.95	33.26	0.78	82.21	28.47	0.47
64J01/B1/W/18	1.67	45.21	1.23	85.52	37.92	0.80
64J01/B2/W/18	1.07	30.74	1.11	72.13	20.88	0.43
64J01/B3/W/18	1.13	37.26	0.83	85.10	24.80	0.57
64J01/C1/W/18	1.23	36.39	1.17	79.53	37.68	0.56
64J01/C2/W/18	1.08	31.46	1.51	74.01	39.74	0.45
64J01/C3/W/18	1.07	36.84	1.06	92.51	23.39	0.57
Min	0.88	30.17	0.55	72.13	20.49	0.42
Max	1.67	45.21	1.51	92.51	39.74	0.80

This publication is licensed under a Creative Commons Attribution 4.0 International License

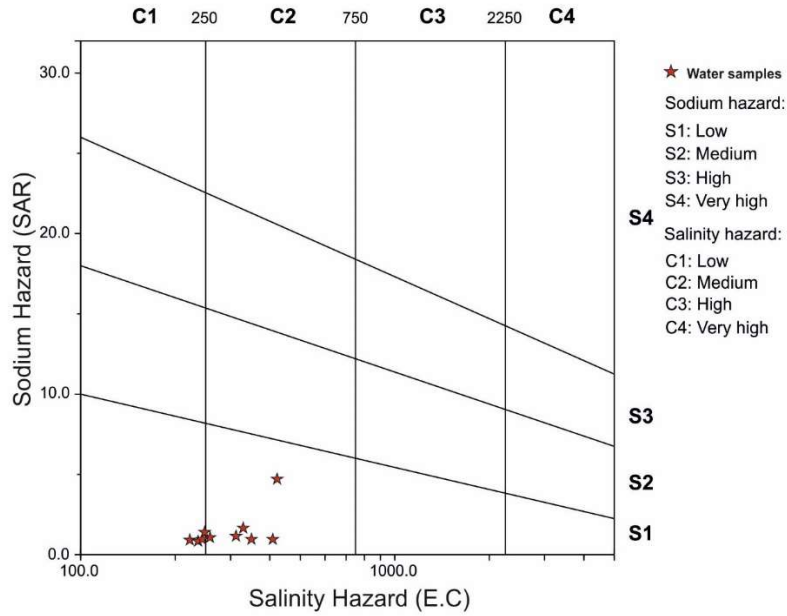

Fig. 9: Classification of irrigation waters using U.S. salinity diagram (USSL 1954).

area, all the surface water samples fall in the excellent category and are suitable for irrigation on almost all soil types with no sodium hazard.

The geochemical parameters of the water samples are plotted in the Salinity Hazards versus Sodium Hazards (USSL) diagram (Richards 1954) to assess the suitability of irrigation water using SAR and EC values. It is a scatter plot of Sodium Hazard (SAR) on the y-axis vs. Salinity Hazard (conductivity) on the x-axis. The sodium hazard of irrigation water is estimated by the sodium absorption ratio (SAR), which is related to the proportion of Na^+ to Ca^{2+} and Mg^{2+} (Kevin 2005). In this plot, the C1 zone represents 'low,' C2 represents 'medium,' C3 represents 'high,' and C4 represents 'very high' salinity hazard. S1 zone represents 'low,' S2 represents 'medium,' S3 represents 'high,' and S4 represents 'very high' sodium hazard. The USSL plot for the study area shows that most water samples have low to medium salinity hazard with low sodium hazard (C2-S1) (Fig 9). Fig. 9 shows that almost all the surface water bodies are suitable for irrigation in most of the soil types.

Another crucial element in assessing the sodium risk and the suitability of water for agricultural use is the sodium percentage (Na%). High Na% irrigation water will increase the exchange of sodium content in the soil, affecting the permeability and texture of the soil (Ghazaryan & Chen, 2016). The sodium percentage values in the study area were calculated by the formula in Eq. 2 (Wilcox 1955) and ranged from 30.17-45.21 % with a medium value of 33.25 % (Table 4). All water sample quality falls in the good to permissible category for irrigation purposes (Wilcox 1955, Ayers & Westcot 1985).

Gupta & Gupta (1987) proposed the residual sodium bicarbonate (RSBC) calculation to assess the suitability of water. The water is considered safe, marginal, and unsatisfactory when the RSBC <5, 5-10, and >10 meq.L^{-1}, respectively (Tanvir Rahman et al. 2017). All the samples followed the satisfactory level of irrigation water.

The permeability index (PI) is also used to determine the suitability of the irrigation water. Long-term exposure to irrigation water containing high sodium, calcium, magnesium, and bicarbonate ions negatively impacts soil permeability (Ravikumar et al. 2011, Srinivasamoorthy et al. 2014). Doneen (1964) introduced the permeability index (PI) for assessing the suitability of irrigation water using Eq. 4. Based on the PI values, the irrigated water can be classified as Class I (>75%), Class II (25-75%) and Class III (<25%). The permeability index of the study area ranges from 72.13 to 92.51%. Only two samples out of nine fall under the Class II category, and the rest belong in the Class I category, indicating that the water is good for irrigation purposes (Table 4).

A higher concentration of Mg ions in water adversely affects the soil quality and crop yield (Shil et al. 2019). Paliwal (1972) developed an index called "magnesium hazard" to assess the adverse effects of magnesium in irrigation water and is calculated as magnesium ratio (MH) using the formula (Eq. 5) (Sundaray et al. 2009, Ravikumar et al. 2011). MH values above 50% adversely affect crop

This publication is licensed under a Creative Commons Attribution 4.0 International License

yield and are unsuitable for irrigation (Sundaray et al. 2009). The magnesium ratio varied from 20.49 to 39.74 (Table 4); thus, all surface water bodies fall under the suitable irrigation category.

A high level of sodium in the water is indicated by Kelly's index, which compares sodium to calcium and magnesium (Kelly 1940) and is calculated using Eq. 6. Water with Kelly's index value less than one (KI < 1) is suitable for irrigation. In contrast, KI>1 indicates excess sodium in water, and KI < 2 indicates sodium deficiency in water (Kelly 1940, Sundaray et al. 2009). In this study, the values of Kelly's index range from 0.42 to 0.80, thus indicating that the water is safe for irrigational purposes.

ACKNOWLEDGMENTS

The authors express their sincere thanks to the Addl. Director General, Central Region, Geological Survey of India, Nagpur, India for providing the opportunity to work in such a natural resourceful area. The authors express their deep sense of gratitude to Shri Prashant P Kalpande, Director (G) for his valuable technical guidance in executing and completing the assigned work. The authors also acknowledge the Geo-data division, SU: CG, Raipur, for providing help in map generation and the Regional Chemical Laboratory, GSI, Nagpur, for the lab support. Finally, sincere thanks to Dr. P.K. Goel, Chief Editor, Nature Environment and Pollution Technology, for providing the opportunity to submit the manuscript and also for his valuable comments and suggestions on this manuscript.

CONCLUSIONS

The study contributes to understanding heavy metals contamination of sediments, soils, and water due to anthropogenic activity, mainly in agriculture-based rural areas. Heavy metals like Pb, Zn, Cu, and Co concentrations in stream sediments/slope-wash samples are higher than their UCC abundance. In contrast, Cr, Cd, Hg, Ni, and Se concentrations are below UCC value. When compared with the globally acceptable permissible or critical limits of each element, it has been observed that the concentration of Pb, Cd, Cu, Hg, and Se is well within safe limits. Slightly higher concentrations are observed in Cr, As, Zn, and Co but not higher than the critical range. The Ni concentration in the area shows maximum values of 47.0 ppm, mainly in the southwestern part. The elements distribution map shows high concentration zones for Ni, Cr, and As over granite and granite gneiss, mainly in the southwestern part. Higher concentrations have also been observed in soil samples, where the bottom C-horizon is more enriched in heavy metals. This higher concentration of Ni-Cr might have come from using phosphatic fertilizer, as agricultural lands occupy all high-value areas. Zn enrichment in the top part of the soil profile in R-horizon in the southern and south-eastern regions also indicates extensive use of fertilizer and soil amendments in the form of poultry and swine manure. Adequate measures should be taken by health and agricultural authorities in these areas for the betterment of the environment and society.

Water quality assessment of major streams in the study areas shows all parameters are well below the permissible limits of drinking water norms. Correlation analysis reveals a poor correlation between sodium and potassium, suggesting the anthropogenic source of sodium in water. Thus, the chemical weathering of rock-forming minerals doesn't control the surface water chemistry of the study area. The estimation of irrigation water quality of the surface water bodies indicates that these stream waters are suitable for irrigation on almost all soil types with no sodium hazard and low to medium salinity hazard.

This study also shows the importance of the country's geochemical mapping database, which will have much broader applications than conventional mineral exploration and geological mapping.

REFERENCES

Abdu, N., Abdullahi, A.A. and Abdulkadir, A. 2017. Heavy metals and soil microbes. Environ. Chem. Lett., 15 (1): 65-84.

Acharyya, S.K. 2003. The nature of the Mesoproterozoic central Indian tectonic zone with exhumed and reworked older granulites. Gondwana Res., 6(2): 197-214.

Alloway, B.J. 1990. Heavy metals in soils. Wiley, New York.

Appleton. J.D. and Ridgway. J. 1992. Regional geochemical mapping in developing countries and its applications to environmental studies. Appl. Geochem. Suppl., 2: 103-110.

Awasthi, S.K. 2000. Prevention of food adulteration Act no 37 of 1954, Central and state rules as amended for 1999. Ashoka Law House, New Delhi.

Ayers, R.S. and Westcot, D.W. 1985. Water quality for agriculture, irrigation, and drainage (Paper No. 29). FAO, Rome.

Bakshi, S., Banik, C. and He, Z. 2018. The Impact Of Heavy Metal Contamination On Soil Health. In: Reicoskey, D. (ed) Managing Soil Health For Sustainable Agriculture. Taylor and Francis, Milton Park, pp. 63-95.

Baltrenaite, E. and Butkus, D. 2004. Investigation of heavy metals transportation from soil to the pine tree. Water Sci. Technol., 50: 239-244.

BIS 1991. Bureau of Indian Standards, 10500 Indian Standard drinking water specification, 1st rev., 1-8.

Central Ground Water Board, 2013. Groundwater brochure of Korba District, Chhattisgarh 2012-2013. Available online: ttps://cgwb.gov.in/District_Profile/Chhatisgarh/Korba.

Chauhan, S., Thakur, R. and Sharma, G. 2008. Nickel: its availability and reactions in the soil. J. Ind. Pollut. Control., 24(1): 1-8.

Chaurasia, A.K., Pandey, H.K., Tiwari, S.K., Pandey, P. and Ram, A. 2021. Groundwater vulnerability assessment using water quality index (WQI) under geographic information system (GIS) framework in parts of Uttar Pradesh, India. Sustain. Water Resour. Manag., 7(3): 1-15.

This publication is licensed under a Creative Commons Attribution 4.0 International License

Chopra, A.K., Pathak, C. and Parasad, G. 2009. The scenario of heavy metal contamination in agricultural soil and its management. J. Appl. Nat. Sci., 1: 99-108.

Comly, H.H. 1945. Cyanosis in infants is caused by nitrates in well water. J. Am. Assoc., 129: 12-114.

Dhirendra, M.J., Kumar, A. and Agrawal, N. 2009. Assessment of the irrigation water quality of river Ganga in Haridwar District. Rasayan. J. Chem., 2: 285-292.

Doneen, L.D. 1964. Notes on water quality in agriculture. Water Science and Engineering, University of California, Davis.

Fetter, C.W. 2001. Applied Hydrogeology. Prentice-Hall, Inc., Hiscock, K.M. (ed), Hydrogeology: Principles and Practice. Blackwell Publishing, London, pp. 436-532.

Ghazaryan, K. and Chen, Y. 2016. Hydrochemical assessment of surface water for irrigation purposes and its influence on soil salinity in Tikanlik Oasis, China. Environ. Earth Sci., 75(5): 383.

Gibbs, R.J. 1970. Mechanism controlling world water chemistry. Sciences, 170: 795-840.

Gupta, S.K. and Gupta, I.C. 1987. Management of Saline Soils and Waters. Oxford and IBH Publishing Company, New Delhi

Hapke, H.J. 1996. Heavy Metal Transfer in the Food Chain to Humans. In Rodriguez-Barrueco, C. (ed), Fertilizers and Environment, Springer, Netherlands, pp. 431-486.

Hashim, M.A., Mukhopadhyay, S., Sahu, J.N. and Sengupta, B. 2011. Remediation technologies for heavy metal contaminated groundwater. J. Environ. Manage., 92(10): 2355-88.

He, Z., Shentu, J., Yang, X., Baligar, V.C., Zhang, T. and Stofella, P.J. 2015. Heavy metal contamination of soils: Sources, indicators, and assessment. J. Environ. Indic., 9: 17-18.

Hem, J.D. 1991. Study and Interpretation of the Chemical Characteristics of Natural Water. Third Edition. Scientific Publishers, Jodhpur, India, pp. 263.

Iimura, K., Ito, H., Chino, H., Morishita, M. and Hirta, H. 1977. The behavior of contaminant heavy metals in the soil-plant system. Proc. Inst. Sem., 11: 357.

Iyaka, Y.A. 2011, Nickel in soils: a review of its distribution and impacts. Sci. Res. Essays, 6(33): 6774-6777.

Jovanović, V.S., Mitić, V., Mandić, S.N., Ilić, M. and Simonović, S. 2015. Heavy Metals in the Postcatastrophic Soils. Sherameti, I. and Varma, A. (eds), Heavy Metal Contamination of Soils: Monitoring and Remediation, Springer International Publishing, New York, pp. 3-21.

Kabata-Pendias, A. 2011. Trace Elements in Soils and Plants. Fourth Edition. CRC Press, New York.

Kabata-Pendias, A. and Mukherjee, A.B. 2007. Trace Elements from Soil to Human. Springer- Verlag, Berlin.

Kabata-Pendias, A. and Pendias, H. 1992. Trace Elements in Soils and Plants. CRC Press, London.

Kaur, M., Soodan, R.K., Katnoria, J.K., Bhardwaj, R., Pakade, Y.B. and Nagpal, A.V. 2014. Analysis of physico-chemical parameters, genotoxicity, and oxidative stress-inducing potential of soils of some agricultural fields under rice cultivation. Trop. Plant Res., 1(3): 49-61.

Kelly, W.P. 1940. Permissible Composition and Concentration of Irrigated Waters. In: Proceedings of the ASCF 66, pp. 607.

Kevin, M.H., 2005. Hydrogeology Principles and Practice. Blackwell Science Ltd., London, pp. 202.

Khalili, M. and Torabi, H. 2003. The exploration of sodium-sulphate in Aran playa, Kashan, central Iran. Carbon. Evap., 18: 120-124.

Kools, S.A.E., Van Roovert, M., Van Gestel, C.A.M. and Van Straalen, N.M. 2005. Glyphosate degradation as a soil health indicator for heavy metal polluted soils. Soil Biol. Biochem., 37(7): 1303-1307.

Krishna, A.K., Rama Mohan, K. and Murthy, N.N. 2011. A multivariate statistical approach for monitoring heavy metals in sediments: a case study from Walipalli watershed, Nalgonda district, Andhra Pradesh, India. Res. J. Environ. Earth Sci., 3(2): 103-113.

Kumar, S.K., Babu, S.H., Rao, P.E., Selvakumar, S., Thivya, C., Muralidharan, S. and Jeyabal, G. 2016. Evaluation of water quality and hydrogeochemistry of surface and groundwater, Tiruvallur District, Tamil Nadu. India Appl. Water Sci., 7(5): 2533-2544.

Maji, A.K., Goon, S., Bhattacharya, A., Mishra, B., Mahato, S. and Bernhardt, H. J. 2008. Proterozoic polyphase metamorphism in the Chhotanagpur Gneissic Complex (India), and implication for transcontinental Gondwanaland correlation. Precamb. Res., 162: 385-402.

Mcllveen, W.D. and Negusanti, J.J. 1994. Nickel in terrestrial environment. Sci. Total Environ., 148: 109-138.

Mohankumar, K., Hariharan, V. and Rao, N.P. 2016. Heavy metal contamination in groundwater around industrial estate vs. residential areas in Coimbatore, India. J. Clin. Diagn. Res., 10(4): BC05-7.

Mushtaq, N. and Khan, K.S. 2010. Heavy metals contamination of soils in response to wastewater irrigation in Rawalpindi region. Pak. J. Agrl. Sci., 47(3): 215-224.

NGCM SOP, 2011. Standard operating procedure for national geochemical mapping. Geological Survey of India, Central Head Quarter, Kolkata.

Notten, M.J.M., Oosthoek, A.J.P., Rozema, J. and Aerts, R. 2005. Heavy metal concentrations in a soil–plant–snail food chain along a terrestrial pollution gradient. Environ. Pollut., 138(1): 178-90.

Oliver, M.A. and Gregory, P.J. 2015. Soil, food security, and human health: A review. Euro. J. Soil Sci., 66(2): 257-76.

Paliwal, K.V. 1972. Irrigation with saline water. Monogram no. 2, new series. IARI, New Delhi, pp. 198.

Pepper, I.L. 2013. The soil health-human health nexus. Crit. Rev. Environ. Sci. Technol., 43(24): 2617-52.

Piper, A.M. 1944. A graphic procedure in the geochemical interpretation of water analysis. Trans. A.G.U., 25: 914-923.

Ramadan, M.A.E. and Al-Ashkar, E.A. 2007. The effect of different fertilizers on the heavy metals in soil and Tomato plants. Aust. J. Basic Appl. Sci., 1(3): 300-306.

Raven, K.P. and Loeppert, R.H. 1977. Trace Element composition of fertilizers and soil amendments. J. Environ. Qual., 26: 551-557.

Ravikumar, P., Somashekar, R.K. and Angami, M. 2011. Hydrochemistry and evaluation of groundwater suitability for irrigation and drinking purposes in the Markandeya River basin, Belgaum District, Karnataka State, India. Environ. Monit. Assess., 173: 459-487.

Rayment, G.E., Jeffery, A.J. and Barry, G.A. 2002. Heavy metals in Australian sugarcane. Commun. Soil Sci. Plant Anal., 33: 3203-3212.

Richards, L.A. 1954. Diagnosis and improvement of saline and alkali soils. Agric Handbook 60, USDA, Washington.

Sarwar, N., Imran, M., Shaheen, M.R., Ishaque, W., Kamran, M.A., Matloob, A., Rehim, A. and Hussain, S. 2017. Phytoremediation strategies for soils contaminated with heavy metals: Modifications and future perspectives. Chemosphere, 171: 710-21.

Shil, S., Singh, U.K. and Mehta, P. 2019. Water quality assessment of a tropical river using water quality index (WQI), multivariate statistical techniques, and GIS. Appl. Water Sci., 9 (7): 168.

Shiow-Mey, L., Shang-Lien, L. and Shan-Hsien, W. 2004. A generalized water quality index for Taiwan. Environ. Monit. Assess., 96: 35-52.

Siamak, G. and Srikantaswamy, S. 2009. Analysis of agricultural impact on the Cauvery River water around KRS dam. World Appl. Sci. J., 6(8): 1157-1169.

Skowron, P., Skowro´nska, M., Bronowicka-Mielniczuk, U., Filipek, T., Igras, J., Kowalczyk-Ju´sko, A. and Krzepiłko, A. 2018. Anthropogenic sources of potassium in surface water: the case study of the Bystrzyca river catchment, Poland. Agric. Ecosyst. Environ., 265: 454-460.

Srinivasamoorthy, K., Gopinath, M., Chidambaram, S., Vasanthavigar, M. and Sarma, V.S. 2014. Hydrochemical characterization and quality appraisal of groundwater from Pungar sub-basin, Tamilnadu, India. J. King Saud. Univ. Sci., 26: 37-52.

This publication is licensed under a Creative Commons Attribution 4.0 International License

Sundaray, S.K., Nayak, B.B. and Bhatta, D. 2009. Environmental studies on river water quality with reference to suitability for agricultural purposes: Mahanadi river estuarine system, India—a case study. Environ. Monit. Assess., 155: 227-243.

Tanvir Rahman, M.A.T.M., Saadat, A.H.M., Islam, M.S., Al-Mansur, M.A. and Ahmed, S., 2017. Groundwater characterization and selection of suitable water type for irrigation in the western region of Bangladesh. Appl. Water Sci., 7: 233-243.

Tchounwou, P.B., Yedjou, C.G., Patlolla, A.K. and Sutton, D.J. 2012. Heavy metals toxicity and the environment. EXS, 101: 133-64.

USSL. 1954. Diagnosis and Improvement of Salinity and Alkaline Soil. USDA Hand Book no. 60, Washington.

Wells, C.R. 1923. Sodium sulfate: Its sources and uses. US Geol. Surv. Bull., 717:11214.

WHO 2011. WHO Guidelines for Drinking-Water Quality, Fourth Edition. World Health Organization, Washington DC.

Wilcox, L.V. 1955. Classification and Use of Irrigation Waters. USDA Circular No. 969, pp. 19.

Wolfgang, W. and Dohler, H. 1995. Heavy Metals in Agriculture. Springer, Germany.

Yang, J., Teng, Y., Wu, J., Chen, H., Wang, G., Song, L., Yue, W., Zuo, R. and Zhai, Y. 2017. Current status and associated human health risk of vanadium in soil in China. Chemosphere, 171: 635-43.

ORCID DETAILS OF THE AUTHORS

Manash Protim Baruah: https://orcid.org/0000-0002-4398-6645

This publication is licensed under a Creative Commons Attribution 4.0 International License